EXTRAPOLATION OF WIND SPEED DATA FOR WIND ENERGY APPLICATIONS

Jennifer F. Newman[1]* and Petra M. Klein[1]
[1]School of Meteorology, University of Oklahoma, Norman, OK

1. INTRODUCTION

Environmental concerns and rising fossil fuel prices have prompted rapid development in the renewable energy sector. Wind energy, in particular, is projected to emerge as one of the fastest-growing renewable energy technologies in the world (U.S. Energy Information Administration 2012). In fact, the U.S. Department of Energy has examined a scenario in which 20% of the energy needs of the U.S. are provided by wind energy by the year 2030 (U.S. DOE 2008). Such a scenario could reduce annual carbon dioxide emissions from the energy sector by 825 million metric tons but would require a large increase in the installed wind capacity in the U.S. (U.S. DOE 2008).

It has been estimated that the Great Plains region possesses the country's highest wind power potential (Fig. 1). The land in the Great Plains is mostly flat and located far away from both ocean coasts; the lack of complex terrain allows wind to flow unimpeded for great distances. These factors, in addition to the prominence of the nocturnal low-level jet, create a vast, largely untapped potential for wind power in the Great Plains. However, wind farm siting is often a meticulous process that requires examining the site's wind climatology at turbine hub heights, which typically range from 60 to 100 m above ground level (AGL) (Schwartz and Elliott 2005). As most standard meteorological observation sites were not designed for wind energy applications, there is a substantial lack of meteorological data at these heights (Petersen et al. 1998b). Thus, researchers and engineers often extrapolate wind speed data from near-surface observation stations to typical hub heights to estimate wind power potential (e.g., Schwartz and Elliott 2005).

Typical extrapolation methods include the use of power laws and the application of Monin-

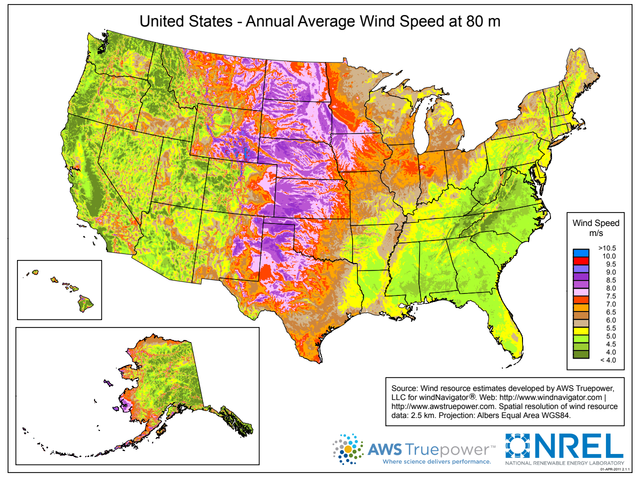

Figure 1: Wind resource map for the United States. From WindPoweringAmerica.gov.

Obukhov similarity theory (Petersen et al. 1998a). However, simple power laws include a single exponent, which can vary with height, stability, and surface roughness (Petersen et al. 1998a). Monin-Obukhov similarity theory assumes that surface fluxes of heat and momentum are constant with height (Arya 2001), an assumption that is generally untrue at night when the boundary layer is stable (Pahlow et al. 2001).

In this work, 10-m wind speed data from the Oklahoma Mesonet and 80-m wind speed data from a tall tower are used to evaluate the power law extrapolation method and two different forms of Monin-Obukhov similarity theory. The gradient Richardson number, calculated from the Oklahoma Mesonet data, is used to separate the wind speed data into stability classes.

2. BACKGROUND

2.1. *Data Sources*

The Oklahoma Mesonet is comprised of over 110 surface observation stations across the state of Oklahoma. Jointly operated by the University

* *Corresponding author address:* Jennifer F. Newman, School of Meteorology, University of Oklahoma, 120 David L. Boren Blvd., Norman, OK 73072.
E-mail: jennifer.newman@ou.edu

of Oklahoma and Oklahoma State University, the Mesonet began network-wide data collection in 1994. Every 5 minutes, each Mesonet site reports standard surface variables, including solar radiation, rainfall, pressure, air temperature, and wind speed. Some Mesonet sites also record soil moisture and temperature at several different levels. Air temperature is measured with thermistors at 1.5 and 9 m AGL. Cup anemometers provide wind speed at 2 m and wind monitors provide wind speed and direction at 10 m (McPherson et al. 2007).

Tall data collection towers in Oklahoma are maintained by the Oklahoma Wind Power Initiative (OWPI), housed at the University of Oklahoma. Several towers were constructed near potential wind farm sites and in some locations, wind instrumentation was added to existing communications towers. Wind speed and direction are collected by cup anemometers and wind vanes at several heights, ranging from 20 m to 80 or 100 m at some of the higher towers. More information can be found on the OWPI website — http://www.ocgi.okstate.edu/owpi/default.asp.

2.2. *Extrapolation Methods*

In this paper, three approaches are used to produce correlations between 10- and 80-m wind speeds.The first approach involves the use of a power law to relate wind speeds at different heights to a reference wind speed at a reference height close to the ground (typically 10 m AGL). The power law that is commonly used in wind energy is defined by the following equation:

$$u(z) = u_{ref}(\frac{z}{z_{ref}})^p$$

where $u(z)$ is the wind speed at height z, u_{ref} is the wind speed at height z_{ref}, and p is the power law exponent. Traditionally, neutral atmospheric conditions have been associated with $p = 1/7$, with values higher (lower) than 1/7 indicating stable (unstable) conditions (Petersen et al. 1998a). High values of the shear exponent indicate that the wind speed changes rapidly with height, which is common in stable regimes when the surface layer is decoupled from the rest of the boundary layer and vertical momentum transport is limited. In contrast, low values of the shear exponent indicate that wind speeds are fairly uniform with height, which is common during unstable regimes with substantial vertical mixing (Garratt 1992).

Monin-Obukhov Similarity Theory (MOST) uses a series of similarity functions to estimate the vertical wind speed profile. The modified "log-law" equation is used to estimate the mean wind speed at different heights, z, AGL:

$$\bar{u}(z) = \frac{u_*}{\kappa}\left(ln\frac{z}{z_o} - \Psi_m(\zeta)\right)$$

u_* is the friction velocity, z_o is the roughness length, and $\Psi_m(\zeta)$ is a function that takes stability into account. ζ is the normalized Obukhov length, z/L, where $L = -\frac{u_*^3\overline{\theta_v}}{\kappa g \overline{w'\theta_v'}}$. $\overline{\theta_v}$ is the mean virtual potential temperature at the measurement height, κ is the von Kármán constant (commonly set as 0.4), g is acceleration due to gravity, and $\overline{w'\theta_v'}$ is the heat flux measured at the surface (Arya 2001). If an eddy-covariance measurement system is available, the heat flux and friction velocity can be estimated and inserted into the Obukhov length equation. If flux measurements are not available, the gradient Richardson number can be used to approximate the non-dimensional Obukhov length (Dyer and Hicks 1970).

One major disadvantage of MOST is that it assumes fluxes are constant with height, which is typically only valid in the surface layer. Gryning et al. (2007) showed that the wind profile based on MOST is only valid up to 50–80 m AGL for a variety of stability conditions and developed a new set of relations to extend the wind profile above the surface layer. This method, referred to as Extended MOST (EMOST) in this paper, uses a set of length scales to estimate the wind speed profile. The characteristic wind profile length scale, l, is related to unique length scales in the surface layer, middle boundary layer, and upper boundary layer in the following equation:

$$\frac{1}{l} = \frac{1}{L_{SL}} + \frac{1}{L_{MBL}} + \frac{1}{L_{UBL}}$$

In the method of Gryning et al. (2007), the following general equation is used to estimate the wind speed profile for different stability conditions:

$$\bar{u}(z) = \frac{u_*}{\kappa}\left(ln\frac{z}{z_o} - \underbrace{\Psi_m(\zeta)}_{Stability} + \underbrace{\frac{z}{L_{MBL}}}_{MiddleBL} - \underbrace{\frac{z}{z_i}\frac{z}{2L_{MBL}}}_{UpperBL}\right)$$

$\Psi_m(\zeta)$ is a parameter that takes stability into account, similar to the stability parameter in MOST, L_{MBL} is the length scale in the middle boundary layer, and z_i is the boundary layer height.

3. WIND SPEED DATA

Wind speed data for the month of August 2011 were used for this study. This month was chosen because the weather is typically quiescent in Oklahoma during the month of August. An analysis of 500-mb height charts during this time period indicated that flow was zonal for most of the month, with a large ridge over much of the Southern Plains. Thus, variations in wind speed were likely influenced primarily by diurnal variations.

Wind speed data at 80 m were obtained from a tall tower in Roger Mills County. Because the data are proprietary, the exact location of the tall tower cannot be disclosed. The Cheyenne Mesonet site, located within 25 km of the tall tower, was used to obtain 2- and 10-m wind speed data, as well as 1.5-m and 9-m temperature. Wind speed data from the tall tower are available in 10-min averages, while Mesonet data are available in 5-min averages. Thus, the 5-min averages from the Mesonet were further averaged to produce 10-min averages to match the tall tower data.

A scatter plot of all the 10-m and 80-m wind speed data for the month of August 2011 is shown in Fig. 2. Although many of the wind speed points are clustered in the same area, there are several outliers that represent a significant amount of wind speed shear. Generally, the 80-m wind speeds were higher than the 10-m wind speeds, although this was not always the case.

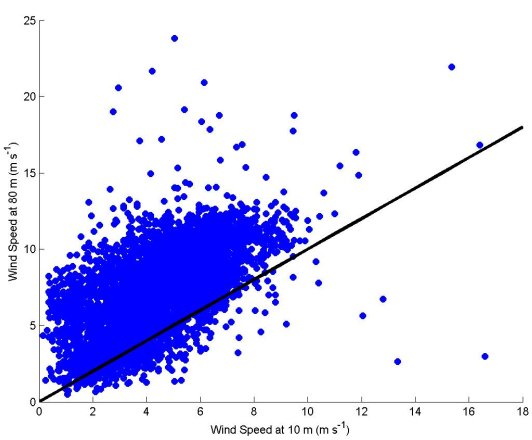

Figure 2: Scatter plot of 10-m wind speeds from the Cheyenne Mesonet site and 80-m wind speeds from a nearby tall tower for the month of August 2011. 1:1 line is shown for reference.

In order to separate the wind speed data into more clearly defined stability regimes, the gradient Richardson number, Ri was calculated. Ri is defined by the following equation:

$$Ri = \frac{g}{T_o} \frac{\frac{\partial \theta}{\partial z}}{(\frac{\partial u}{\partial z})^2}$$

where g is the gravitational acceleration, T_o is the surface temperature, and $\frac{\partial u}{\partial z}$ and $\frac{\partial \theta}{\partial z}$ are the vertical gradients of wind speed and potential temperature, respectively. In this study, Ri was calculated from the Cheyenne Mesonet station following the method of Bodine et al. (2009):

$$Ri = \frac{g[(T_{9m} - T_{1.5m})/\Delta z_T + \Gamma_d)]\Delta z_u^2}{T_{1.5m}(u_{10m} - u_{2m})^2}$$

where T_{9m} and $T_{1.5m}$ are the temperatures at 9 and 1.5 m AGL, respectively, u_{10m} and u_{2m} are the wind speed magnitudes at 10 and 2 m AGL, respectively, and Δz_T and Δz_u refer to the differences in measurement levels for T and u. The vertical gradient of potential temperature is approximated by adding the dry adiabatic lapse rate, Γ_d, to the temperature gradient. Ten-minute averages of the wind speed and temperature data were used to calculate a different value of Ri for every 10 min of observations.

In this work, stability classifications were loosely based on the classifications of Mauritsen and Svensson (2007) and defined as follows:

Strongly unstable: $Ri < -0.2$
Unstable: $-0.2 \leq Ri < -0.1$
Neutral: $-0.1 \leq Ri < 0.1$
Stable: $0.1 \leq Ri < 0.25$
Strongly stable: $Ri \geq 0.25$

According to these classifications, 22% of the wind speed data pairs during August 2011 occurred during a strongly unstable regime, 7.6% occurred during an unstable regime, 30.3% occurred during a neutral regime, 30.5% occurred during a stable regime, and 9.6% occurred during a strongly stable regime.

A scatter plot of 10- and 80-m winds stratified by stability classification is show in Fig. 3. The unstable 10-m wind speed observations appear to be approximately linearly correlated with the 80-m wind speed observations; in fact, many of the unstable observations are located near the 1:1 line. This makes sense, since unstable atmospheres often have well-mixed, uniform profiles of wind speed (Garratt 1992). In contrast, most of the observations corresponding to stable conditions are located above the 1:1 line, indicating that 80-m wind speeds are higher than 10-m wind speeds and wind shear exists in the vertical direction.

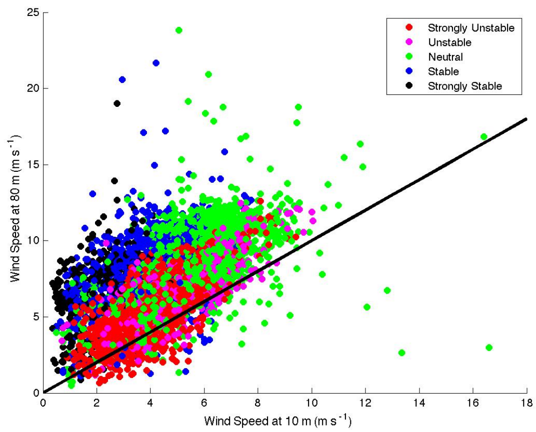

Figure 3: As in Fig. 2, but different stability classifications are indicated by colored circles.

4. EXTRAPOLATION METHODS: RESULTS

In this section, the 10- and 80-m wind speed data for the month of August 2011 are fit to a power law. In addition, Monin-Obukhov similarity theory and the extended Monin-Obukhov similarity theory of Gryning et al. (2007) are used to predict the 80-m wind speeds for the various stability classes. The accuracy of these extrapolation methods is explored for different stability regimes.

4.1. *Power Law*

First, the wind speed data were used to fit a power law of the form $u(z) = u_{ref}(\frac{z}{z_{ref}})^p$. u_{ref} was taken to be the wind speed measured at 10 m by the Cheyenne Mesonet site, as 10 m is a common reference level used to fit the power law in wind energy studies (Petersen et al. 1998a). The statistics toolbox in MATLAB was used to fit a linear regression to the wind speed data, and a best-fit line of the form $u(80m) = u(10m) * slope$ was found. For the power law, the slope is equal to $(z/z_{ref})^p$. Solving for p gives $p = ln(slope)/ln(z/z_{ref}) = ln(slope)/ln(80m/10m)$. Different values of p were calculated for the different stability classes, then used to calculate 80-m wind speeds from 10-m wind speeds.

Values of the coefficient of determination, R^2, and shear exponent, p, for the power law fit are shown in Table 1. The values of p are lower than the neutral value of 1/7 (= 0.143) for unstable conditions and greater than 1/7 for stable conditions. In addition, the value of p approximated from the wind speed data increases with increasing stability, as expected (Petersen et al. 1998a).

Scatter plots for the power law fit are shown in Fig. 4. The power law fit the strongly unstable, unstable, neutral, and stable regime wind speed data very well, with R^2 values exceeding 0.9 (Figs. 4a–d). However, the power law did not fit the strongly stable regime wind speed data as well, producing an R^2 value of 0.826 (Fig. 4e).

4.2. *Monin-Obukhov Similarity Theory*

Next, the 10-m wind speeds were used to find the Monin-Obukhov similarity functions at each observation time, and a modified log-law equation was used to estimate the 80-m wind speeds. The process to compute the similarity functions largely follows the gradient method outlined in Arya (2001).

First, the non-dimensional height, $\zeta = z/L$, was calculated from the gradient Richardson number using the following equations:

$$\zeta_m = \frac{z_m}{L} = Ri; Ri < 0$$
$$\zeta_m = \frac{z_m}{L} = \frac{Ri}{1-5Ri}; 0 \leq Ri < 0.2$$

where z_m is the mean geometric height used for the calculation of Ri. For this work, z_m was taken as $\sqrt{10m * 2m} = 4.47m$. Although Ri in the gradient method is typically calculated assuming logarithmic profiles for wind speed and temperature, the previously-calculated value of Ri was used for simplicity.

Next, the Obukhov length, L, was calculated by dividing z_m by ζ_m. Values for ζ at 10 and 80 m were calculated by dividing the heights of 10 and 80 m by the Obukhov length. The similarity functions for momentum at 10 and 80 m were obtained from the Businger-Dyer relations:

$$\phi_m = (1 - 15\zeta)^{-1/4}; -5 < \zeta < 0$$
$$\phi_m = 1 + 5\zeta; 0 \leq \zeta < 1$$
$$\Psi_m = -5\zeta; \zeta \geq 0$$
$$\Psi_m = 2ln(\frac{1+x}{2}) + ln(\frac{1+x^2}{2}) - 2tan^{-1}(x) + \frac{\pi}{2}; \zeta < 0$$

where $x = (1 - 15\zeta)^{1/4}$.

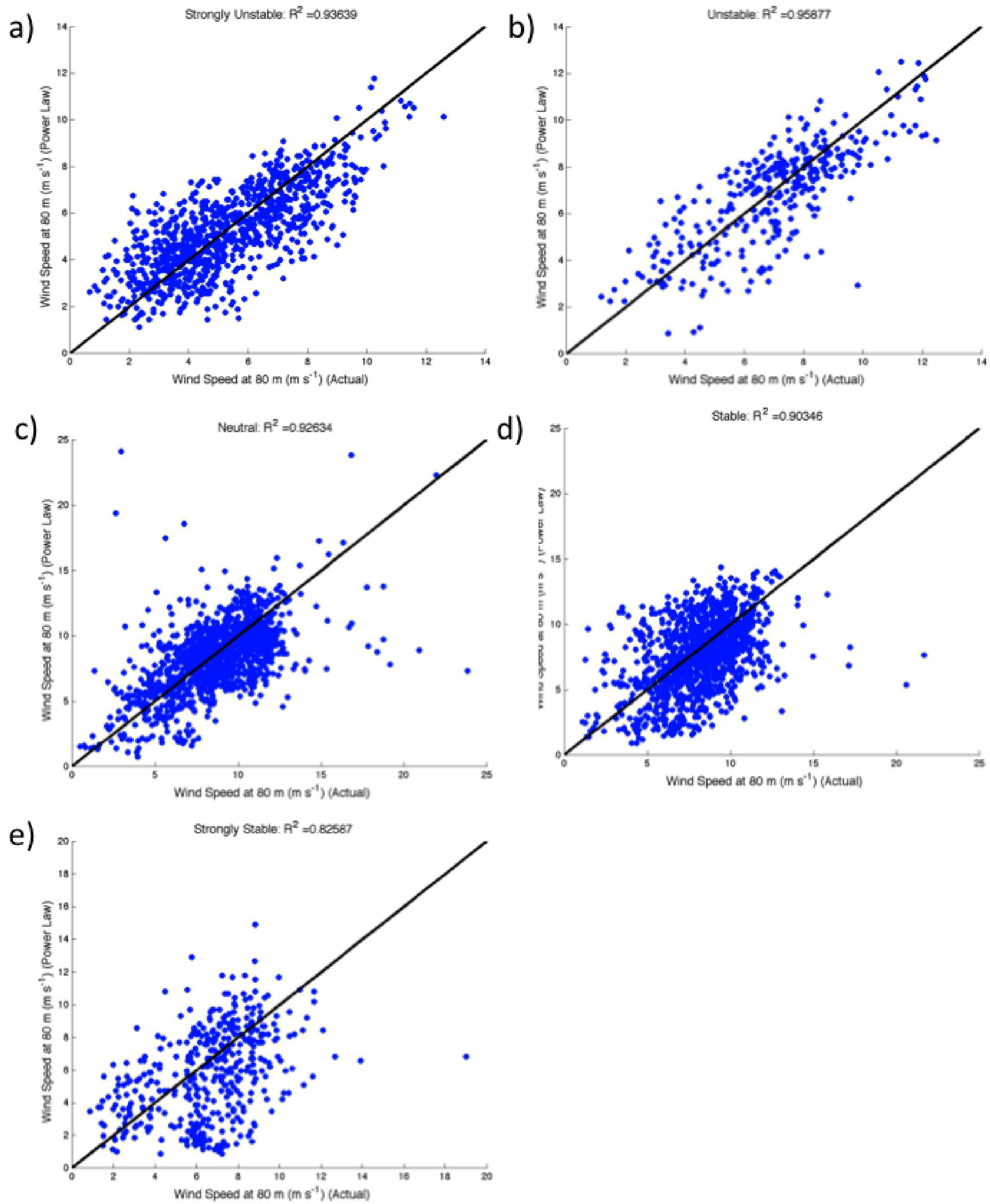

Figure 4: Estimated 80-m wind speeds from power law fit compared to true 80-m wind speeds for a) strongly unstable b) unstable c) neutral d) stable and e) strongly stable regimes. Observation/estimation pairs are indicated by blue circles and 1:1 line is shown by thick black line for reference.

The friction velocity, u_*, was found through the equation for the dimensionless wind speed gradient:

$$\left(\frac{\kappa z}{u_*}\right)\left(\frac{\partial \bar{u}}{\partial z}\right) = \phi_m\left(\frac{z}{L}\right)$$

For this work, z was set to z_m in the equation above, κ was set to 0.4, and the derivative of u with respect to z was found using a finite-difference approach, assuming a logarithmic wind profile:

$$\frac{\partial \bar{u}}{\partial z} = \frac{u_{10m} - u_{2m}}{ln(\frac{10m}{2m})z_m}$$

Mean values of u_* were approximately 0.3 m s^{-1}. Next, the roughness length, z_o, was calculated by assuming a modified log-law profile for the wind speed:

$$\bar{u}(z) = \frac{u_*}{\kappa}\left(ln\frac{z}{z_o} - \Psi_m(\zeta)\right)$$

Values for $\bar{u}$ and $\Psi_m(\zeta)$ at 10 m were used to solve for z_o. Mean values of z_o derived from the data were approximately 0.03 m, which is fitting for the open fields near the Cheyenne Mesonet site (Stull 2000). Finally, the calculated values of u_*, z_o, and $\Psi_{m(80m)}$ were used to calculate the wind speed at 80 m from the modified log-law equation outlined above.

Results from the Monin-Obukhov similarity theory method are shown in Fig. 5. (Note that the Monin-Obukhov method assumes a maximum Ri of 0.2, so similarity theory was not applied to the strongly stable regime wind speeds.) Similarity theory produced fairly good results for the strongly unstable, unstable, and neutral regimes ($R^2 > 0.9$); the observation/estimation pairs were scattered somewhat evenly about the 1:1 line, indicating that similarity theory produced approximately equal numbers of overestimates and underestimates of the 80-m wind speed (Figs. 5a–c). However, many of the similarity theory estimates were inaccurate for the stable regime (R^2 = 0.692; Fig. 5d).

The stable regime wind speeds estimated from MOST appear to be separated into two groups: several estimates are scattered below the one-to-one line, while several more estimates are scattered above the one-to-one line. It is possible that these two separate groups of wind speed estimates are related to different degrees of stability. This would not be surprising, considering the varying amount of wind shear between the 10-m stable regime wind speeds and the corresponding 80-m wind speeds (Fig. 3). In general, the inaccuracy of Monin-Obukhov similarity theory for the stable regime is likely related to the underlying assumptions of the theory. Monin-Obukhov similarity theory assumes that heat and momentum fluxes are uniform with height (Arya 2001), which is likely not true when the boundary layer is stable and highly stratified (e.g., Pahlow et al. 2001).

4.3. *Extended Monin-Obukhov Similarity Theory*

Finally, the EMOST method of Gryning et al. (2007) was used to estimate 80-m wind speeds for different stability regimes. By using different length scales for different parts of the boundary layer, Gryning et al. (2007) show that the wind speed profile in neutral conditions can be determined through the following equation:

$$\bar{u}(z) = \frac{u_*}{\kappa}\left(ln\frac{z}{z_o} + \frac{z}{L_{MBL,N}} - \frac{z}{z_i}\frac{z}{2L_{MBL,N}}\right)$$

$L_{MBL,N}$ is the length scale in the middle boundary layer under neutral conditions. By using tower observations, Gryning et al. (2007) determine an empirical fit for $L_{MBL,N}$, given by:

$$L_{MBL,N} = \frac{u_{*o}}{f}/(-2ln\frac{u_{*o}}{fz_o} + 55)$$

where f is the Coriolis parameter.

The estimated wind profiles for stable and unstable conditions include a correction factor for stability. The stable wind profile is given by the following equation:

$$\bar{u}(z) = \frac{u_*}{\kappa}\left(ln\frac{z}{z_o} + \frac{bz}{L}(1 - \frac{z}{2z_i}) + \frac{z}{L_{MBL}} - \frac{z}{z_i}\frac{z}{2L_{MBL}}\right)$$

In this paper, the constant b was set to 5, following the Dyer and Hicks (1970) method.

Similarly, the wind profile for unstable conditions is given by the following equation:

$$\bar{u}(z) = \frac{u_*}{\kappa}\left(ln\frac{z}{z_o} - \Psi(\frac{z}{L}) + \frac{z}{L_{MBL}} - \frac{z}{z_i}\frac{z}{2L_{MBL}}\right)$$

where $\Psi(\frac{z}{L}) = \frac{3}{2}ln\frac{1+x+x^2}{3} - \sqrt{3}tan^{-1}(\frac{1+2x}{\sqrt{3}}) + \frac{\pi}{\sqrt{3}}$ and $x = (1 - 12z/L)^{1/3}$. For stable and unstable conditions, Gryning et al. (2007) determined the following empirical relation for L_{MBL}:

$$L_{MBL} = \frac{u_{*o}}{f}/((-2ln\frac{u_{*o}}{fz_o} + 55)exp(-\frac{u_{*0}/fL}{400}))$$

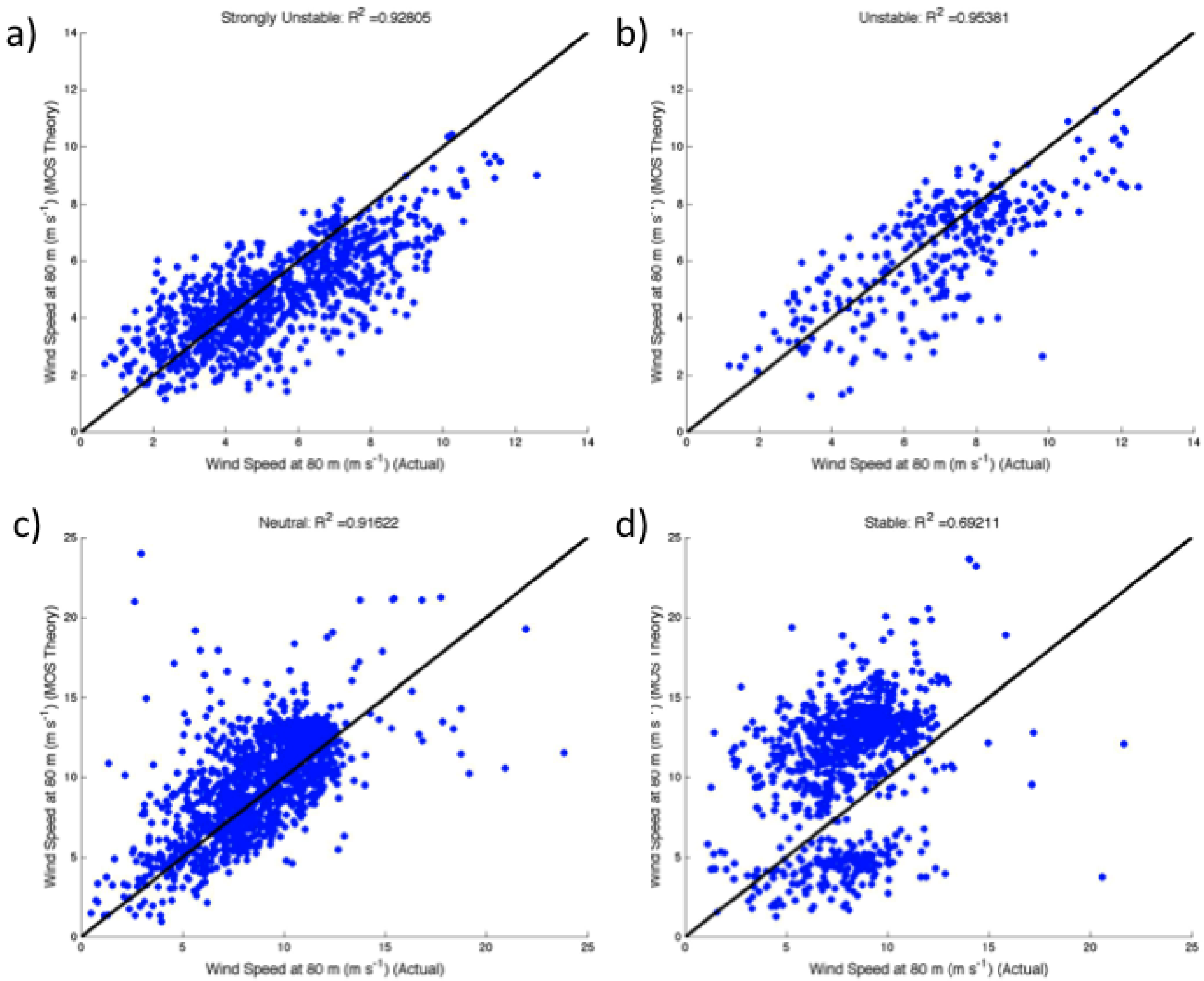

Figure 5: Estimated 80-m wind speeds from Monin-Obukhov similarity theory compared to true 80-m wind speeds for a) strongly unstable b) unstable c) neutral and d) stable regimes. Observation/estimation pairs are indicated by blue circles and 1:1 line is shown by thick black line for reference.

Values of u_* and z_o were determined the same way they were determined for MOST in the previous section.

One of the parameters in the EMOST wind profile equations is the boundary layer height, z_i. Gryning et al. (2007) estimate the mean boundary layer height for different stability regimes by examining heat and momentum fluxes from sonic anemometers on a tower and extrapolating the flux measurements upward. However, sonic anemometers are not available on either the tall tower or the Mesonet station, so a simple parameterization for the boundary layer height was used in this paper. Gryning et al. (2007) suggest that the approximation $z_i \approx 0.1 u_{*o}/f$ be used when the boundary layer height is not known, so this approximation was adopted for the present study.

The wind profile estimation results from the EMOST method are shown in Fig. 6. Similar to the MOST estimates, the 80-m wind speed estimates from EMOST were most accurate for strongly unstable, unstable, and neutral regimes. However, the EMOST wind speed estimates for stable regimes are significantly closer to the observed 80-m wind speeds (R^2 = 0.896) in comparison to the MOST estimates (R^2 = 0.692). In addition, unlike the MOST estimates, the EMOST wind speed estimates are not separated into different groups for the stable regime wind speeds (Fig. 6d). Thus, there does seem to be a slight advantage to using the extended Monin-Obukhov Similarity Theory of Gryning et al. (2007), at least for stable regime wind speed estimates.

5. Summary and Conclusions

In this work, 10-m wind speed data from the Cheyenne Mesonet site and 80-m wind speed data from a nearby tall tower were used to evaluate different wind speed extrapolation techniques. The gradient Richardson number was calculated from the Mesonet data and used to separate the wind speed data into five different stability classes: strongly unstable, unstable, neutral, stable, and strongly stable.

The R^2 values for the different extrapolation methods and stability regimes are shown in Table 1. The results for all three methods were similar for the strongly unstable, unstable, and neutral regimes, although R^2 values were slightly higher for the power law method for all three regimes. Monin-Obukhov Similarity Theory produced the lowest R^2 value for the stable regime wind speed data, and also appeared to separate the extrapolated wind speed data into two different groups (Fig. 5d). The discrepancy in R^2 values for the stable regime wind speed data is likely the result of the assumptions of similarity theory; as previously discussed, MOST assumes that surface fluxes are constant with height, which is generally untrue for stable regimes.

As tall tower data were also available at 31, 50, and 65 m, mean wind speed profiles produced by the extrapolation methods can be compared to the actual mean wind speed profiles observed at the tall tower. The mean wind speed profiles produced by the extrapolation techniques are shown in Fig. 7 and mean estimation errors are shown in Fig. 8. The power law method produced good fits for the strongly unstable and unstable regime wind speed data. This is not surprising, as wind speeds tend to be well-mixed in unstable boundary layers and highly correlated at different heights (Garratt 1992). However, the power law method produced poor results for the strongly stable and stable regimes, likely because wind speeds in the stable boundary layer are often highly sheared and turbulence and momentum transport are weak and intermittent (Garratt 1992). The power law tended to underestimate, on average, the 80-m wind speeds for the stable and strongly stable regimes (Figs. 7a, 8a), suggesting that the power law does not adequately capture the amount of vertical wind shear present in stable atmospheric regimes. However, the mean wind speed error produced by the power law method was within +/- 2 m s^{-1} for all heights and stability regimes (Fig. 8a).

Both the MOST and the EMOST fit overestimated wind speeds for the stable regimes, but produced fairly accurate estimates for the strongly unstable and unstable regimes (Figs. 7b,c, 8b,c). For the MOST fit, the stable regime wind speed error increases with height (Fig. 8b), suggesting that similarity theory becomes less and less valid with increasing height. In contrast, the EMOST errors for the stable regime are relatively constant with height (Fig. 8c).

In conclusion, extrapolation methods that use Monin-Obukhov Similarity Theory only appear to produce accurate wind speed estimates for unstable regimes. The extended similarity theory developed by Gryning et al. (2007) requires the use of several additional approximations and parameterizations, but could produce better wind speed estimates for stable regimes in comparison to traditional Monin-Obukhov Similarity Theory. Surprisingly, the most simple method in this paper, the power law method, appeared to produce the smallest mean wind speed errors for all heights and stability regimes. This method does not make any assumptions about stability or constant fluxes in the surface layer. However, the shear parameter in the power law is highly dependent on atmospheric stability, and is likely location-dependent as well.

The power law was also the only method that directly used 80-m wind speeds in the extrapolation fit. While the shear exponents for the power law fit were derived from the wind shear between 10 and 80 m, the parameters in the MOST and EMOST fits were solely determined from the 2- and 10-m Mesonet observations. Furthermore, MOST, unlike the power law, assumes that wind speed increases logarithmically with height in the surface layer; this assumption was invalid whenever the 10-m wind speeds were larger than the 80-m wind speeds, which was true for some portions of the study time period (Fig. 2). These discrepancies could have influenced the superior performance of the power law in comparison to MOST and EMOST.

In the future, more complex, non-linear methods such as neural networks (Bishop 1995) could be explored to produce better fits for wind speeds in the stable boundary layer. More stability and wind shear parameters may need to be integrated in order to relate 10-m wind speeds to 80-m wind speeds in the stable boundary layer. In addition, 80-m wind speeds could be integrated into the

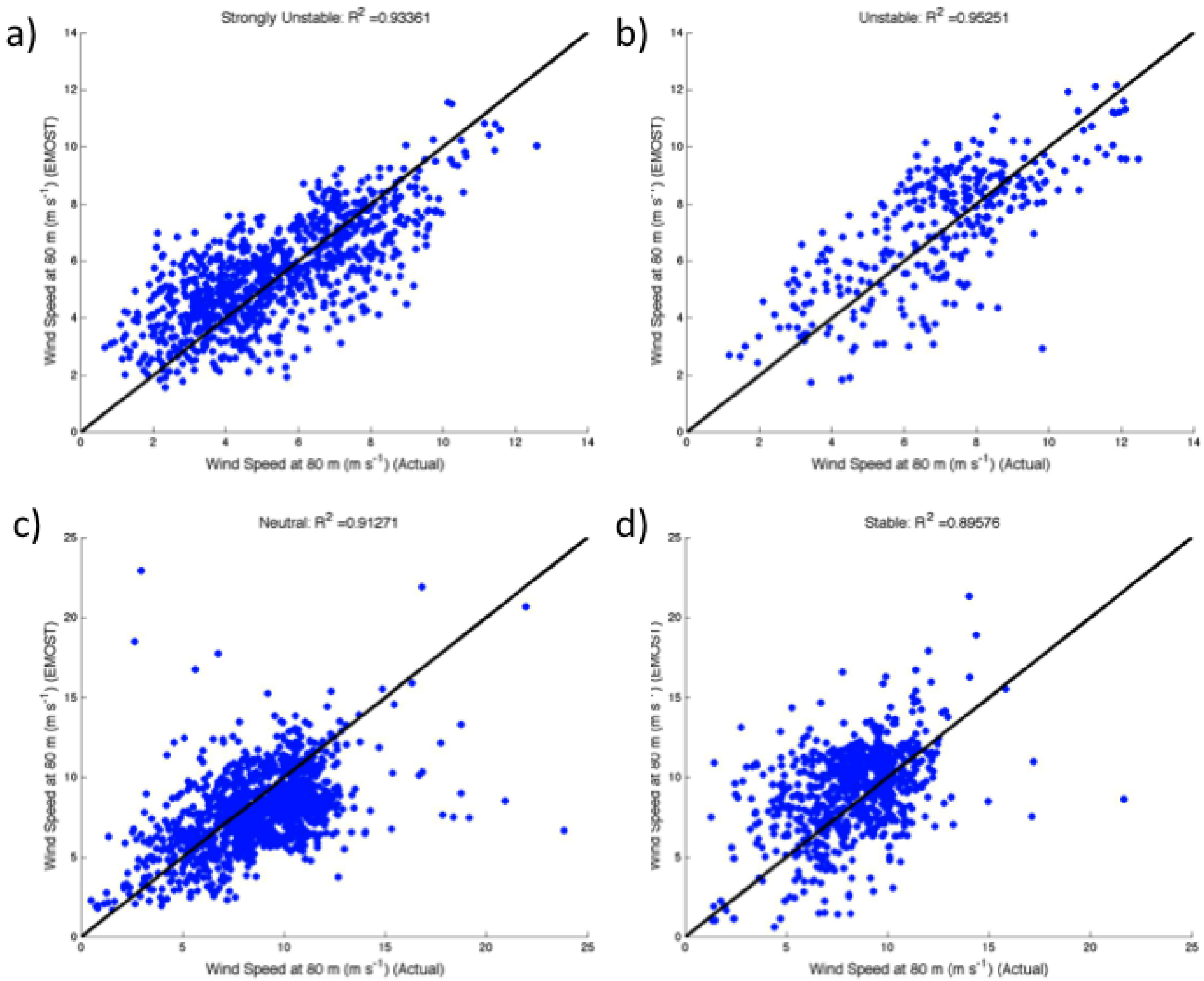

Figure 6: Estimated 80-m wind speeds from extended Monin-Obukhov similarity theory compared to true 80-m wind speeds for a) strongly unstable b) unstable c) neutral and d) stable regimes. Observation/estimation pairs are indicated by blue circles and 1:1 line is shown by thick black line for reference.

Method	Strongly Unstable	Unstable	Neutral	Stable	Strongly Stable
Power Law	0.936 (p = 0.108)	0.959 (p = 0.105)	0.926 (p = 0.179)	0.903 (p = 0.288)	0.826 (p = 0.438)
MOST	0.928	0.954	0.916	0.692	-
EMOST	0.934	0.953	0.913	0.896	-

Table 1: Coefficient of determination (R^2) values for different extrapolation methods and stability classes. For power law results, value of shear exponent, p, is shown in parentheses.

MOST and EMOST methods to provide more fair comparisons to the power law method.

6. ACKNOWLEDGMENTS

The authors would like to thank Michael Klatt at the Oklahoma Wind Power Initiative for his assistance in obtaining tall tower data.

7. REFERENCES

Arya, S. P., 2001: *Introduction to Micrometeorology*. Academic Press, 420 pp.

Bishop, C. M., 1995: *Neural Networks for Pattern Recognition*. Oxford University Press, New York, NY, 482 pp.

Bodine, D., P. M. Klein, S. C. Arms, and A. Shapiro, 2009: Variability of surface air temperature over gently sloped terrain. *J. Appl. Meteor. Climatol.*, **48**, 1117–1141.

Dyer, A. J. and B. B. Hicks, 1970: Flux-gradient relationships in the constant flux layer. *Quarterly Journal of the Royal Meteorological Society*, **96**, 715–721.

Garratt, J., 1992: *The Atmospheric Boundary Layer*. Cambridge University Press, 316 pp.

Gryning, S.-E., E. Batchvarova, B. Brümmer, H. Jørgensen, and S. Larsen, 2007: On the extension of the wind profile over homogeneous terrain beyond the surface boundary layer. *Boundary-Layer Meteorology*, **124**, 251–268.

Mauritsen, T. and G. Svensson, 2007: Observations of stably stratified shear-driven atmospheric turbulence at low and high Richardson numbers. *J. Atmos. Sci.*, **64**, 645–655.

McPherson, R. A. and Coauthors, 2007: Statewide monitoring of the mesoscale environment: A technical update on the Oklahoma Mesonet. *J. Atmos. Oceanic Technol.*, **24**, 301–321.

Pahlow, M., M. Parlange, and F. Porté-Agel, 2001: On Monin–Obukhov similarity in the stable atmospheric boundary layer. *Boundary-Layer Meteorology*, **99**, 225–248.

Petersen, E. L., N. G. Mortensen, L. Landberg, J. Højstrup, and H. P. Frank, 1998a: Wind power meteorology. Part I: Climate and turbulence. *Wind Energy*, **1**, 25–45.

Petersen, E. L., N. G. Mortensen, L. Landberg, J. Højstrup, and H. P. Frank, 1998b: Wind power meteorology. Part II: Siting and models. *Wind Energy*, **1**, 55–72.

Schwartz, M. and D. Elliott, 2005: Towards a wind energy climatology at advanced turbine hub-heights. Preprints, *15th Conf. on Applied Climatology*, Savannah, GA. Amer. Meteor. Soc., JP1.9.

Stull, R. B., 2000: *Meteorology for Scientists and Engineers*. 2d ed., Brooks Cole, 528 pp.

U.S. DOE, 2008: 20% wind energy by 2030: Increasing wind energy's contribution to U.S. electricity supply. DOE/GO-102008-2567, 226 pp. [Available online at www.nrel.gov/docs/fy08osti/41869.pdf.].

U.S. Energy Information Administration, 2012: Annual energy outlook 2012. DOE/EIA-0383(2012), 252 pp. [Available online at http://www.eia.gov/forecasts/aeo/pdf/0383(2012).pdf].

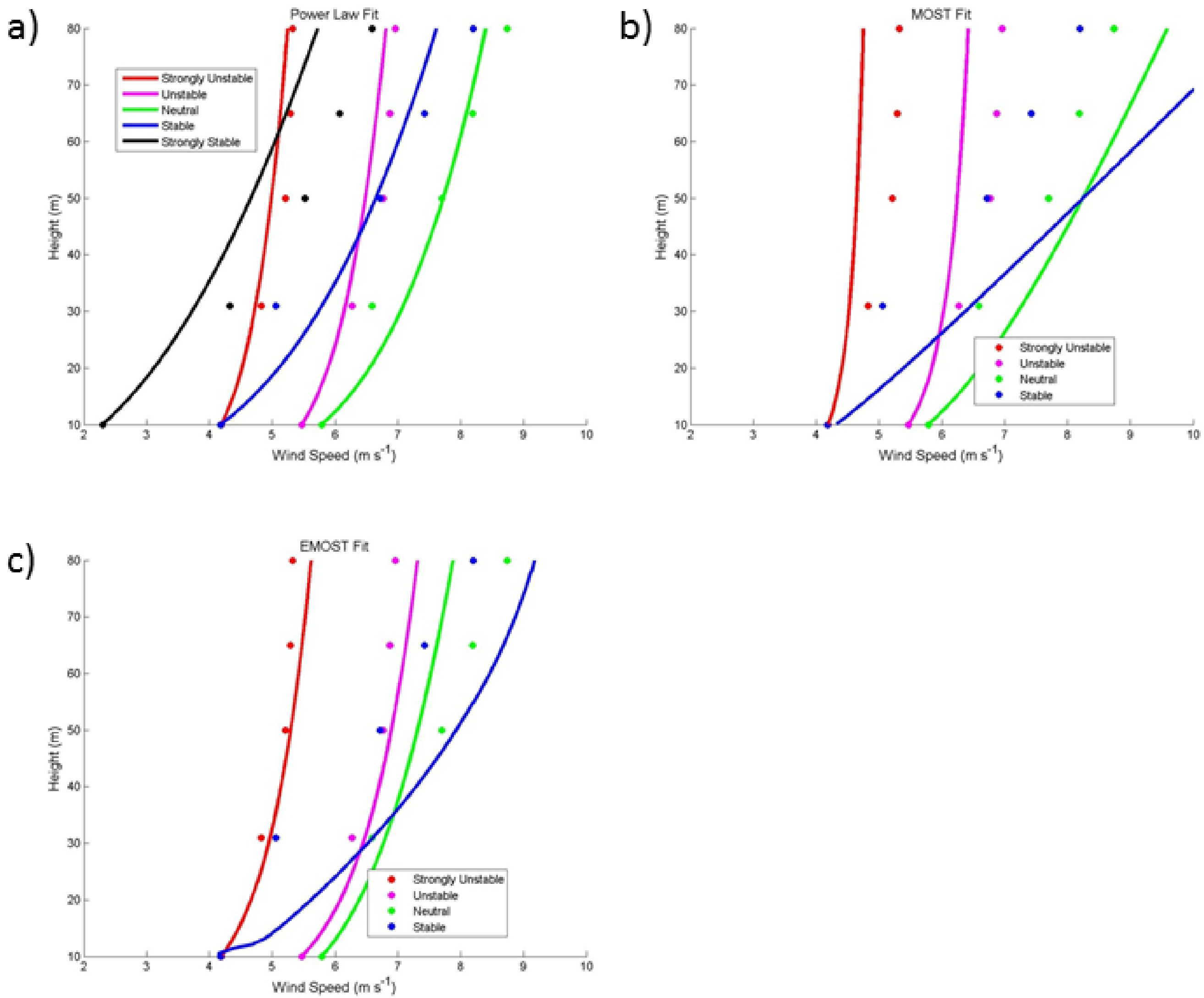

Figure 7: Mean wind speed profiles produced by different extrapolation techniques. Estimated profiles are denoted by solid lines and tall tower observations are denoted by circles.

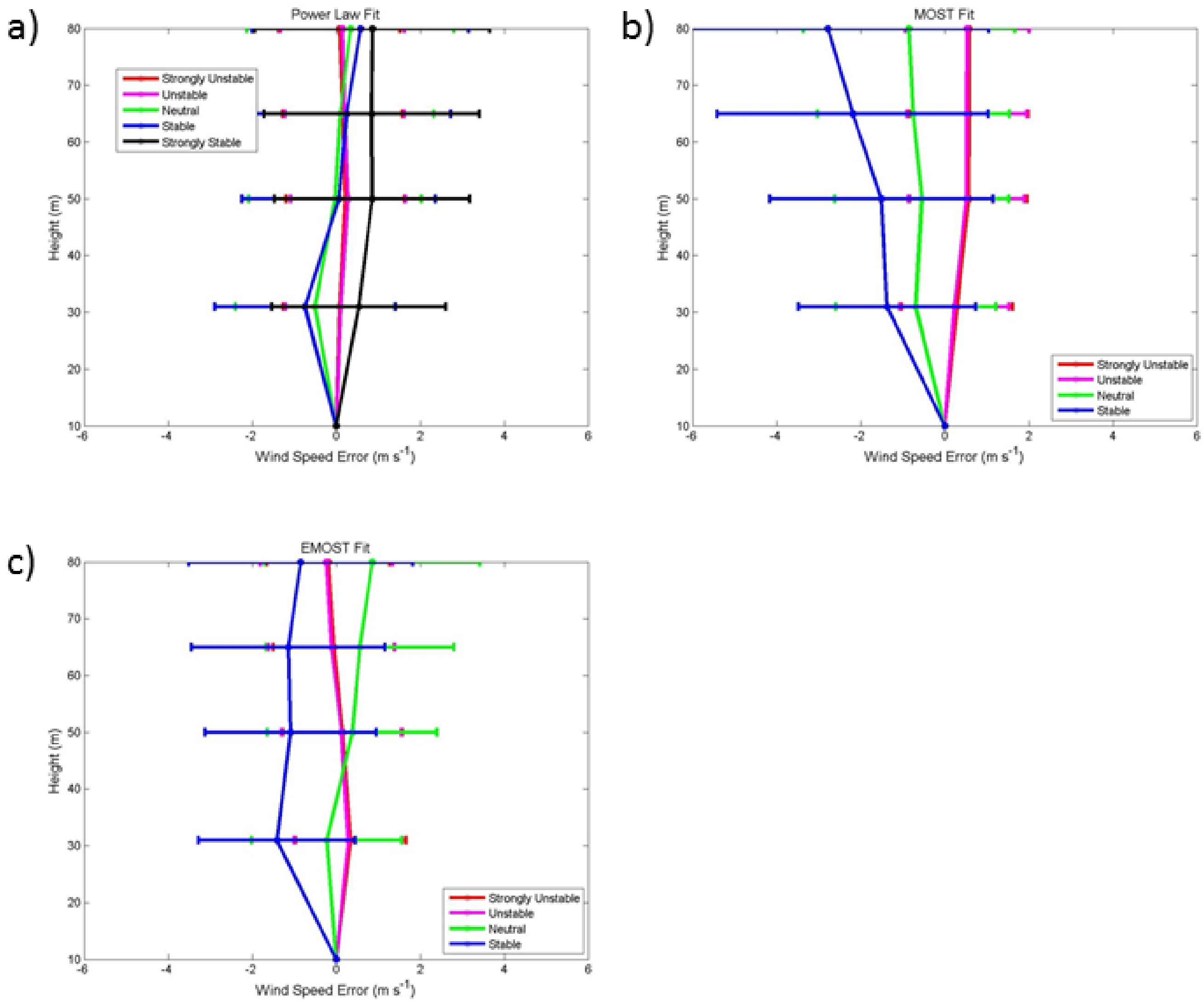

Figure 8: Mean wind speed error profiles for different extrapolation techniques. Error profiles are denoted by solid lines and error bars and and tall tower observations are denoted by circles.